

Anisotropic Collective Flow of Λ -Hyperons Produced in C + C Collisions at 4.2 AGeV/ c

L. Chkhaidze,^{1,*} P. Danielewicz,^{2,†} T. Djobava,^{1,‡} L. Kharkhelauri,¹ and E. Kladnitskaya³

¹*Institute of High Energy Physics and Informatization,
Tbilisi State University, Tbilisi, Georgia*

²*National Superconducting Cyclotron Laboratory,
Michigan State University, East Lansing, Michigan, USA*

³*Joint Institute for Nuclear Research, Dubna, Russia*

Abstract

Features of anisotropic collective flow and spectral temperatures have been determined for Λ hyperons emitted from C + C collisions, at incident momentum of 4.2 AGeV/ c , measured using the Propane Bubble Chamber of JINR at Dubna. Moreover, characteristics of protons and of negative pions, emitted from those collisions, have been determined and provided for comparison. The directed and elliptic flows of Λ s both agree in sign with the corresponding flows of protons. Parameters of the directed and elliptic flows for Λ s agree further, within errors, with the corresponding parameters for the co-produced protons. This contrasts an earlier finding by the E895 Collaboration of the directed flow being significantly weaker for Λ s than protons, in the much heavier Au + Au system, at comparable incident momentum. Particle spectral temperatures in the C + C collisions have been determined focusing independently on either center-of-mass energy, transverse energy or transverse momentum distributions. For either protons or negative pions, the temperatures were found to be approximately the same, no matter whether the emission of those particles was associated with Λ production or not. Results of the measurements have been compared to the results of simulations within the Quark-Gluon String Model.

*Electronic address: ichkhaidze@yahoo.com; Electronic address: ida@hepi.edu.ge

†Electronic address: danielewicz@nscl.msu.edu

‡Electronic address: Tamar.Djobava@cern.ch; Electronic address: djobava@hepi.edu.ge

I. INTRODUCTION

Produced strange particles represent important probes of high-density nuclear matter formed in relativistic heavy-ion collisions. Thus, because of the production thresholds, strangeness needs to be generated within early stages of a collision. Due to their longer mean free path, the strange particles are additionally likely to leave the colliding system earlier than other hadrons. Given the necessary contributions of the early high-density stages of a collision, to the strangeness production, the yields of strange particles have been linked theoretically to the nuclear equation of state of dense matter [1] and to the in-medium modifications of particle masses [2]. In drawing concrete conclusions on the equation of state from yield data, comparison of the results from light C + C and heavy Au + Au systems turned out to be of crucial importance [3]. Further in the literature, the collective-flow characteristics of strange particles, such as of Λ hyperons to be investigated here, were shown [4, 5] to be sensitive to the optical potentials for those particles. For Λ s, the flow characteristics were shown [5, 6], on the other hand, to be relatively insensitive to the Λ -nucleon cross-sections. In the beam-energy of 2–10 AGeV, significant supranormal densities are reached in the collisions [7], accompanied by a good degree of equilibration in heavy systems, conducive for studying the equation of state or optical potentials. In this context, E895 Collaboration has measured yields and directed-flow characteristics of strange particles [8], i.e. Λ hyperons and K^0 and K_s^0 mesons, in the semicentral Au + Au collisions in the beam-energy range of 2–6 AGeV, at the AGS accelerator of the Brookhaven National Laboratory. For Λ s, they have observed a lower flow than for protons, decreasing from $\sim 2/3$ to $\sim 1/3$ of the proton flow, across the 2–6 AGeV range. The experience [3] from the lower energy-range of 0.6–1.5 AGeV has clearly demonstrated, though, that results on strangeness from a light system, where a nontrivial equation of state might seem redundant, can be just as important for learning about bulk nuclear properties, as results from a heavy system such as Au + Au.

In this paper, we present experimental results on characteristics of Λ hyperons produced in the light-system C + C collisions at incident momentum of 4.2 AGeV/ c , registered in the 2 m Propane Bubble Chamber (PBC-500) of JINR. We concentrate on anisotropic-flow characteristics and on spectral temperatures and compare our results for Λ -hyperons to those for protons and π^- mesons from the C + C collisions. We also examine spectral temperatures

of protons and π^- mesons produced in association with Λ hyperons. The anisotropic flows of protons and of π^- mesons have been studied before, on their own, in the C-induced collisions at 4.2–4.5 AGeV/ c in Dubna, specifically by the PBS-500 and the SKM-200-GIBS Collaborations in the semicentral C + C collisions [9] and in the central C + Ne and C + Cu collisions [10, 11].

In the next section, we address the details of our measurements. Thereafter, we discuss the determination of the mean reaction-plane component of Λ transverse-momentum, as a function of Λ rapidity. In Section IV, we discuss the analysis of differential Λ azimuthal-distribution and the determination of Λ elliptic flow parameter. Temperatures of Λ 's, protons and π^- mesons are addressed in Section V. When presenting different experimental results, comparisons are made to the results of Quark-Gluon String Model [12, 13]. Our conclusions are presented in Section 6.

II. EXPERIMENTAL DATA

For the experiment, the 2-m Propane Bubble Chamber (PBC-500) of JINR has been placed in the magnetic field of 1.5 T. Technical details behind the separation of C + C collisions in propane, identification of charged pions and protons, application of different corrections and data processing, may be found in [14]. Here, we concentrate on the identification of Λ hyperons.

The films from PBC-500 exposures have been scanned for V^0 events. In a preliminary examination, the events that either obviously represented e^+e^- pairs or did not point towards the nuclear interaction vertex were rejected. The remaining events were measured in detail and reconstructed. Specifically, the V^0 events were tested, through fits, whether they fulfilled the kinematic conditions for Λ , $\bar{\Lambda}$, K_s^0 decay or γ conversion. Finally, when a V^0 event was deemed to be the charged-particle decay, $\Lambda \rightarrow p + \pi^-$, the momentum of the hyperon was reconstructed from decay products. The procedure resulted in 873 reconstructed Λ -hyperons. For studying the collective flow of Λ s, an exclusive analysis of the collision with an identified hyperon was required.

Depending on the analysis region, for a variety of reasons, some Λ particles with charged decays could not be identified. Specifically, we estimate that about 26% of the particles have been lost because their decay occurred outside of the chamber effective region or too close,

$l < 2$ cm, to the creation vertex. Identification efficiency further deteriorated for certain azimuthal directions, leading to a loss of about 14% of the particles. Finally, about 9% of the particles have been lost in the forward c.m. hemisphere, for directions too close to the beam. Depending on the momentum region, corrections have been applied to the identified particles, in the form of weights, compensating for the losses. Additional information, on the Λ -hyperon identification and on the corrections, can be found in Ref. [15].

For the further analysis, the C + C interactions have been selected, where, aside from a Λ , at least 4 participant protons have been identified. In separating out the participant from fragmentation products, the following criteria have been adopted: $p > 3.5$ GeV/ c and $\Theta < 3^\circ$ for projectile fragmentation and $p < 0.25$ GeV/ c for target fragmentation. It should be mentioned that events with Λ s may contain an admixture of K^+ mesons; the average K^+ multiplicity is, in fact, half of the Λ multiplicity. These are difficult to separate from proton and they contaminate the proton sample, but on the average at the level of less than 10%.

III. DIRECTED FLOW OF Λ HYPERONS

In determining the directed transverse flow of Λ hyperons and of co-produced protons, we have employed the method of Danielewicz and Odnyc [16]. Most of the data below 4 AGeV in the literature have been, in fact, analyzed following that method. The advantage of that method is that it can be employed even at small event statistics, such as typical for film detectors. The method relies on the summation over transverse momentum vectors of selected particles in the events.

The reaction plane is spanned by the impact parameter vector \vec{b} and the beam axis. Within the transverse momentum method [16], the direction of \vec{b} is estimated, event-by-event, in terms of the vector \vec{Q} constructed from particle transverse momenta \vec{p}_i^\perp :

$$\vec{Q} = \sum_{i=1}^n \omega_i \vec{p}_i^\perp, \quad (1)$$

where the sum extends over all protons in an event. The summation weight is $\omega_i = 1$ for $y_i > y_c + \delta$, $\omega_i = -1$ for $y_i < y_c - \delta$ and $\omega_i = 0$ for $y_c - \delta < y_i < y_c + \delta$, where y_i is particle rapidity and y_c is the system c.m. rapidity. Particles around the c.m. rapidity, with weak correlations with the reaction plane, are not included in the reaction-plane determination. In conducting the analysis in the c.m. system, we have $y_c = 0$. Otherwise, in suppressing

the contribution from midrapidity particles to the plane determination, we have employed $\delta = 0.2$.

When referring a specific particle to the reaction plane, we exclude the contribution from that particle to the estimate of the plane, to prevent an auto-correlation. When referring a proton, we exclude that proton; when referring a lambda, we exclude the daughter proton. The reference transverse vector for particle j ($j > n$ for Λ s and daughter protons) is then

$$\vec{Q}_j = \sum_{\substack{i=1 \\ i \neq j}}^n \omega_i \vec{p}_i^\perp, \quad (2)$$

where $i \neq j$ indicates exclusion of the aforementioned contribution and n is the number of primary protons identified in a collision. Projection of the transverse momentum of particle j onto the estimated reaction plane is

$$p_j^{x'} = \frac{\vec{p}_j^\perp \cdot \vec{Q}_j}{|\vec{Q}_j|}. \quad (3)$$

The average in-plane momentum components $\langle p^{x'}(y) \rangle$ can be obtained by averaging, over events, the momenta in different rapidity intervals.

In a small system, such as ours, effects of transverse-momentum conservation in using (2) might be a source of concern [17, 18]. However, when the vector \vec{Q} is dominated by particles with sizeable transverse momenta, that are detected with comparable efficiencies in the forward and backward hemispheres of a symmetric system, then the effects of conservation largely cancel between the hemispheres [17]. A secondary effect is that of momentum conservation spreading out not only over initially present nucleons, but also produced pions.

Due to finite number of protons used in constructing the vector \vec{Q} in (1), the estimated reaction plane fluctuates in the azimuth around the direction of the true reaction plane. Because of those fluctuations, the average momenta $\langle p^{x'} \rangle$, calculated with the estimated reaction plane, get reduced as compared to those for the true reaction plane $\langle p^x \rangle$:

$$\langle p^{x'}(y) \rangle = \langle p^x(y) \rangle \langle \cos \Phi \rangle. \quad (4)$$

Here, Φ is the angle between the true and estimated reaction plane. The overall correction factor $k = 1/\langle \cos \Phi \rangle$, which needs to be applied to $\langle p^{x'}(y) \rangle$, in order to obtain $\langle p^x(y) \rangle$, is subject to uncertainty, especially at low multiplicities. In this work, we evaluate $\langle \cos \Phi \rangle$

from the ratio [16, 19]:

$$\langle \cos \Phi \rangle = \frac{\langle \omega p^{x'} \rangle}{\langle \omega p^x \rangle} = \left\langle \frac{\omega \vec{p}_j^\perp \cdot \vec{Q}_j}{|\vec{Q}_j|} \right\rangle \bigg/ \left(\frac{\langle Q^2 - \sum_{i=1}^n (\omega p_i^\perp)^2 \rangle}{\langle n^2 - n \rangle} \right)^{1/2}. \quad (5)$$

For the ensemble of C + C collisions where a Λ hyperon has been identified, we find $\langle \cos \Phi \rangle = 0.893$ and $k = 1.12$.

Besides looking at the proximity of $\langle \cos \Phi \rangle$ to 1, the accuracy of the reaction-plane determination may be tested by applying the procedure proposed in Ref. [16]. Following that procedure, we have divided randomly each analyzed collision event into two sub-events and we have constructed vectors \vec{Q}_1 and \vec{Q}_2 for those sub-events. The resulting distribution of reaction-plane directions from the sub-events peaks at zero degrees in relative azimuthal angle and it exhibits a width of $\sigma \approx 50^\circ$. This peaking directly testifies to the presence of the special azimuthal direction in the events. The distribution of reaction planes determined from full events, about the true reaction-plane direction, should be about half as wide as the relative distribution of directions from the sub-events [16, 20]. The thus-estimated spread of the estimated reaction-plane directions about the true plane direction, $\sigma_0 \simeq \sigma/2 = 25^\circ$, is comparable to the values reported in [21] and to the values of $\sigma_0 \approx 23 \div 25^\circ$ arrived at in Kr- and Au-induced collisions with Ag(Br) targets [22].

Figure 1 shows the rapidity dependence of the average in-plane transverse-momentum component, from Eq. (3) and corrected for $\langle \cos \Phi \rangle$, for Λ hyperons in panel (a) and for protons co-produced with Λ s in (b). It is apparent that the hyperons and protons flow in the same in-plane directions, in the forward and backward hemispheres of C + C collisions at 4.2 AGeV/c. The dependencies $\langle p^x(y) \rangle$ are rather similar, even in detail, for protons and Λ s, with the magnitude of average momentum either similar for the two species or an edge higher for protons.

In the outer rapidity regions, the values of $\langle p^x(y) \rangle$ for protons may be affected by the longer-term dynamics of nuclear spectator remnants, albeit rather reducing than enhancing proton momenta in their magnitude. One common measure, quantifying the dependence of $\langle p^x \rangle$ on rapidity, away from the spectators, is the slope [23] of $\langle p^x(y) \rangle$ at midrapidity:

$$F = \left. \frac{d\langle p^x \rangle}{dy} \right|_{y=0}. \quad (6)$$

To determine the slopes, marked with straight lines in the panels (a) and (b) of Fig. 1, odd third-order polynomials have been fitted to the data in the midrapidity ranges of $|y| < 0.65$

for Λ s, and $|y| < 0.75$ for protons co-produced with the Λ s. The obtained flow parameters are $F = 99 \pm 15 \text{ MeV}/c$ for Λ s, and $F = 108 \pm 11 \text{ MeV}/c$ for protons co-produced with Λ s. The value of flow for all protons from the 10441 analyzed semi-central C + C collision-events is $F = 113 \pm 10 \text{ MeV}/c$.

Our C + C system is the lightest in the literature for which a directed flow of the Λ -hyperons has been observed. In spite of the system mass, the flow magnitude is similar to that observed for Λ s in other systems within the specific energy regime. Prior measurements of Λ flow have been done by the E895 Collaboration at AGS [8], by the FOPI Collaboration at GSI [24], and by the EOS Collaboration at LBL [25]. In Au + Au collisions, the E895 Collaboration obtained the Λ flow of $F = 140 \pm 35$, 85 ± 15 , and $65 \pm 5 \text{ MeV}/c$, at energies of 2, 4, and 6 AGeV, respectively. The EOS Collaboration measured the flow of Λ s of $F = 85 \pm 43 \text{ MeV}/c$ in Ni + Cu collisions at 2 AGeV. The E895 results indicate a decline of the Λ flow on the high-end side of this energy regime. This decline likely reflects a reduction in time that the initial nuclei spend passing by each other. Determination of $\langle p^x \rangle$ for Λ hyperons emitted from Ni + Ni collisions at 1.93 AGeV, by the FOPI Collaboration, has been done with a $p^\perp/m > 0.5$ cut on the Λ transverse momenta. Therefore, their results are more difficult to compare to those from other measurements. However, within the FOPI data [24], the results for Λ s and protons have been similar, after analogous cuts were applied to the particles.

Interestingly, while the directed flow is similar for Λ s in our C + C system and in the E895 Au + Au system at the comparable beam momentum of 4.8 AGeV/c at the energy of 4 AGeV, this is not the case for protons, whether or not co-produced with the Λ s. Thus, for all protons in Au + Au collisions, the E895 Collaboration has obtained [26] flow parameter values of $F = 238 \pm 15$, 205 ± 19 , and $183 \pm 16 \text{ MeV}/c$, at energies of 2, 4, and 6 AGeV, respectively. The E895 results for protons co-produced with Λ s in Au + Au [8] have been similar. The Au + Au proton flow decreases across the energy range, but not as fast as the Λ flow. Importantly, at the comparable incident momentum per nucleon to ours, of 4.8 AGeV/c, the proton flow is about twice as high in Au + Au than in our C + C system, while the Λ flow is similar. This points to possible differences in the origin of the flow of protons and Λ hyperons in the Au + Au and C + C systems, such as in a greater mean-field contribution to the proton flow in Au + Au.

Theoretically, the Λ flow has been described in the past within the ARC cascade

model [27] that produced the value of $F = 113 \pm 31 \text{ MeV}/c$ [25] for the Ni + Cu collisions at 2 AGeV. At the same time, the relativistic transport model RVUU [4] produced the value of $F = 96 \pm 17 \text{ MeV}/c$ for those collisions [25]. In spite of differences in the details of those models, within the errors they both reproduce the 2 AGeV results. Within the RVUU model, the Λ mean-field potential has been fairly weak [5]. The RQMD model [28], with no mean field for Λ s, produced Λ -flow that was consistent with E895 Au + Au data at 2 AGeV and underestimated the data at 4 AGeV.

Our own measurements [29] from the collisions involving carbon, as either projectile or target, have been compared in the past to the predictions of the Quark-Gluon String Model (QGSM). This model combines string fragmentation with a hadronic cascade. A detailed description of QGSM can be found in Refs. [12, 13]. Using the COLLI Monte-Carlo generator [30] based on QGSM, we have generated 7578 inelastic C + C collision events, at the incident momentum of 4.2 AGeV/ c , where the production of Λ hyperons has been recorded. When selecting participant protons, the same rejection criteria have been applied as to the protons in the experiment. In addition, from the analysis, the protons with deep angles, greater than 60° , have been excluded, because experimental efficiency for detecting such steep tracks is greatly reduced. In the analysis of Λ flow, only events with 4 or more participant protons were utilized. The average Λ and co-produced proton in-plane momenta are shown, together with the data, in Fig. 1. It is apparent that the model describes the data in a semi-quantitative manner. Values of the flow parameter, determined within the QGSM model, are $F = 97 \pm 8 \text{ MeV}/c$ and $F = 108 \pm 8 \text{ MeV}/c$, for the Λ s and for co-produced protons, respectively.

IV. ELLIPTIC FLOW OF Λ HYPERONS

In the midrapidity region, where the directed flow is suppressed and the net particle abundance is the highest, another form of emission anisotropy persists, of elliptic type. It is associated with the geometry of the reacting system in purely transverse directions. The overlap region of initial nuclei has an elliptic shape, and in this is more elongated out of the reaction plane than in the plane. The resulting pressure gradients are stronger in the in-plane than out-of-plane directions, producing initially a stronger collective flow in the reaction plane direction than out of the plane. However, the spectator matter present in the

vicinity of the reaction zone can suppress the growth of collective motion within the plane, yielding in the end a stronger elliptic collective flow out of the plane, commonly termed squeeze-out.

At high enough energies, the spectator matter moves away from the reaction zone quickly enough, though, to permit the growth of in-plane flow, which then prevails. Our incident energy is, actually, close to the energy where the transition in the direction for the elliptic flow occurs. Also, an elliptic emission pattern can be produced by pure mean-free-path effects [31]. With Λ s likely emitted over a shorter time than are emitted protons, the mean-free-path effects could produce a stronger out-of-plane elliptic pattern for Λ s than for protons. In such a small system as ours, obviously, the mean-free-path effects have a greater chance to play a prominent role than in a heavier system.

To gain an insight into the midrapidity emission pattern, we plot in Fig. 2 the distribution of Λ hyperons (panel (a)), and of co-produced protons (panel (b)), in the azimuthal angle relative to the reaction plane. The angle for particle j is obtained from $\cos \varphi_j = p_j^{x'}/p_j^\perp$ and we lump together the left and right sides of the reaction plane, in order to increase statistics. To emphasize the emission patterns, the ordinate axes do not start at zero in Fig. 2.

As is seen in Fig. 2, both the Λ and co-produced proton distributions peak at 90° , i.e. out of the reaction plane, exhibiting squeeze-out that is characteristic for lower incident energies, where the spectator remnants modify the emission. The two patterns in Fig. 2 are actually quite similar; approximately the two distributions differ just by an overall normalization factor of about 3.35. The distributions, however, tend to be flattened by the fluctuations of the estimated reaction plane about the true reaction plane. To better quantify the anisotropies, we fit the distributions with the function

$$\frac{dN}{d\varphi} = a_0 (1 + a'_1 \cos \varphi + a'_2 \cos 2\varphi) . \quad (7)$$

For squeeze-out, the coefficient a'_2 is negative. Compared to the coefficient a_2 , associated with a distribution relative to the true reaction plane, a'_2 is reduced, though, by [32, 33]

$$a'_2 = a_2 \langle \cos 2\Phi \rangle , \quad (8)$$

in an analogy to the reduction in (4). The reduction coefficient for (8) may be estimated from [29]

$$\langle \cos 2\Phi \rangle = \frac{|\langle (p^{x'})^2 - (p^{y'})^2 \rangle|}{|\langle (p^x)^2 - (p^y)^2 \rangle|} , \quad (9)$$

where the numerator and denominator on the r.h.s. are, respectively, obtained from

$$\langle (p^{x'})^2 - (p^{y'})^2 \rangle = \left\langle 2 \left(\frac{\vec{p}_j^\perp \cdot \vec{Q}_j}{Q_j} \right)^2 - (p_j^\perp)^2 \right\rangle, \quad (10)$$

and

$$|\langle (p^x)^2 - (p^y)^2 \rangle| = \sqrt{\frac{\langle 2\bar{\bar{T}} : \bar{\bar{T}} - \sum_{i=1}^n (p_i^\perp)^4 \rangle}{\langle n^2 - n \rangle}}. \quad (11)$$

In the above, the transverse tensor $\bar{\bar{T}}$ is

$$T^{\alpha\beta} = \sum_{i=1}^n \left(p_i^\alpha p_i^\beta - \frac{1}{2} (p_i^\perp)^2 \delta^{\alpha\beta} \right), \quad \alpha = x, y, \quad (12)$$

and

$$\bar{\bar{T}} : \bar{\bar{T}} = \sum_{\alpha, \beta=x}^y T^{\alpha\beta} T^{\alpha\beta} = (T^{xx})^2 + (T^{yy})^2 + 2(T^{xy})^2. \quad (13)$$

Use of Eq. (9), for a reaction, requires that some elliptic anisotropy is present in the analyzed system to start with, which, obviously though, is the case given the results in Fig. 2. With Eq. (9), using protons only, we find for our system $\langle \cos 2\Phi \rangle \simeq 0.581$. The fits to the azimuthal distributions with Eq. (7) are illustrated with solid lines in Fig. 2. Upon correcting the elliptical-modulation coefficients, following Eq. (8), we obtain $a_2 = -0.062 \pm 0.031$ for Λ -hyperons and $a_2 = -0.049 \pm 0.018$ for the co-produced protons. Within errors, those modulation patterns are similar.

We further compare our elliptic-flow results to the results from the QGSM model of the reaction. The distributions relative to the reaction plane, obtained in the model following experimental procedures, and normalized according to the data, are overlaid over the data in Fig. 2. The corresponding coefficient values are $a_2 = -0.058 \pm 0.017$ for the Λ hyperons (panel (a)) and $a_2 = -0.047 \pm 0.008$ for co-produced protons (panel (b)). As is apparent, the model predicts a clear signature of squeeze-out, the out-of-plane elliptic flow. Further, within the experimental data, the model describes the elliptic-flow data.

Given the proximity of masses for protons and Λ -hyperons, the similarity of directed and elliptical flows for Λ -hyperons and for associated protons could be principally understood in terms of a folding of local thermal distribution with a field of collective velocity. This kind of explanation normally assumes a local grand-canonical ensemble with a universal temperature. However, the production of strangeness could tax the locally available energy and affect the universality of temperature, particularly in such a small system as ours. We next examine thermal characteristics of particle spectral distributions.

V. SPECTRAL TEMPERATURES

In the following, we shall examine the thermal characteristics of spectral distributions of Λ hyperons and of protons and negative pions either co-produced, or not, with the hyperons. The distributions can principally result from a superposition of local thermal distributions and collective velocity field at freeze-out. Obviously, pure thermal distributions cannot explain the asymmetries associated with the reaction plane, that we have discussed. However, here, we shall not attempt to separate those possible collective and locally thermal contributions in a folding. Rather, we shall examine whether the effective temperatures, that could be associated with the distributions, depend on species, on associated production and on the method of analysis of the distribution.

Two primary types of collective motion may have a principal practical impact onto the spectral distributions. Thus, an incomplete stopping of initial nuclei, or transparency, gives rise to a longitudinal collective motion. In addition, collective expansion may develop in a reaction and be reflected in significant transverse radial flow. In the following, we shall examine both the spectral distributions in the net c.m. energy and in the transverse momentum or transverse mass. The latter distributions are less likely to be affected by the longitudinal collective motion than the first. Moreover, we shall explore the potentially different conclusions when confronting data with different versions of the thermodynamic model, such as with the Hagedorn model, assuming particle freezeout within a net c.m. volume common for all particles, and with a model of thermal transverse distribution. First, we analyze particle distributions in the net energy, in terms of the standard thermal model of freeze-out with the c.m. system.

For a gas in thermal equilibrium within the volume V , the distribution in momentum of different species i is [34–36]:

$$\begin{aligned} \frac{d^3 N_i}{dp^3} &= \frac{(2S_i + 1)V}{(2\pi)^3} \left[\exp\left(\frac{E_i - \mu_i}{T}\right) \pm 1 \right]^{-1} \\ &\rightarrow \frac{(2S_i + 1)V}{(2\pi)^3} \exp\left(\frac{\mu_i - m_i}{T}\right) \exp\left(-\frac{E_{Ki}}{T}\right), \end{aligned} \quad (14)$$

where V represents the freeze-out volume, S_i is spin, μ_i is chemical potential, T is temperature, $E_i = \sqrt{m_i^2 + p^2}$ is the particle energy, and $E_{Ki} = E_i - m_i$ is the kinetic energy. The \pm signs refer to fermions and bosons, respectively, and the arrow indicates the Boltzmann-statistics limit of $E_i - \mu_i \gg T$. In a nondegenerate system, the distribution is

then exponential in the kinetic energy, with the temperature T determining the slope of the exponential,

$$\frac{d^3 N}{dp^3} = \frac{d^2 N}{p^2 dp d\Omega} = \frac{d^2 N}{pE dE d\Omega} = \text{const} \cdot \exp\left(-\frac{E_K}{T}\right). \quad (15)$$

Correspondingly, following the global freeze-out model, we can extract the freeze-out temperature by fitting an exponential to the scaled distribution of particles in energy:

$$F(E_K) = (pE)^{-1} dN/dE_K = \text{const} \cdot \exp(-E_K/T). \quad (16)$$

Figure 3 shows the scaled distribution F for Λ s in the rapidity region of $|y| < 0.6$. In addition, Figs. 4 and 5 show, respectively, the distribution for protons at $|y| < 0.6$ and π^- mesons at $|y| < 0.8$, either emitted in the presence or absence of Λ s. In each case, the scaled distributions are quite well described by an exponential. The only significant deviations are observed for the lowest-energy π^- mesons and these deviations likely combine the Coulomb effects and effects of baryon-resonance decays. Temperatures from fits to the kinetic-energy spectra are next provided in Table I. The temperatures are similar, but not the same, for different species. For Λ s, we find the temperature of $T = 111 \pm 7$ MeV, which is higher than the temperature for π^- mesons of the order of 85 MeV, and is lower than the temperature for protons of the order of 134 MeV. A lower spectral temperature for pions than for baryons might be associated with collective motion that has more effect on the more massive baryons than on pions. The difference between protons and Λ s could be principally due to the effects of transparency, that should be of greater importance for the protons than for hyperons produced centrally. In examining, in particular, this last possibility, we next turn to transverse spectra.

The Hagedorn Thermodynamic Model [37, 38] allows, principally, for a set of fireballs displaced from each other in rapidity. In that model, particles with different momenta freeze-out within a volume that is of universal magnitude when assessed in the rest-frame for any given momentum. In that model, the distribution in transverse momentum is of the shape

$$dN/dp^\perp = \text{const} \cdot p^\perp m^\perp K_1(m^\perp/T) \simeq \text{const} \cdot p^\perp (m^\perp T)^{1/2} \exp(-m^\perp/T), \quad (17)$$

where K_1 is the MacDonald function [39], the transverse mass is $m^\perp = \sqrt{m^2 + p^{\perp 2}}$ and the approximation above is valid for $m^\perp \gg T$. For large m^\perp in different thermal models, the scaled distribution in transverse mass is exponential in the mass:

$$F_\alpha(m^\perp) = (m^\perp)^{-\alpha} dN/dm^\perp = \text{const} \cdot \exp(-m^\perp/T), \quad (18)$$

with the Hagedorn model of Eq. (17) being one example where $\alpha = 3/2$. In the following, we shall fit the transverse spectra either using the Hagedorn model or following Eq. (18) with $\alpha = 2$, in order to explore model sensitivity. We will display those fits, respectively, in the context of spectra presented as distributions in transverse momentum, Eq. (17), or scaled distribution in transverse mass, Eq. (18). The two distributions emphasize different parts of the spectrum.

In different panels, Figs. 3, 4 and 5 present the transverse distributions, and the aforementioned fits to those distributions, respectively, for Λ -hyperons and for protons and π^- mesons, either produced in the presence or absence of Λ s. It is apparent that thermal descriptions work also well for the transverse spectra. The temperatures deduced from transverse spectra are provided in Table I. The temperatures for baryons are similar to those deduced from distributions in the c.m. kinetic energy, contradicting the supposition that the latter distributions may be significantly affected by transparency. Greater differences in deduced temperature values are found for the π^- mesons. This may be due to the combination of nonthermal features of spectra, rapidity cut, and nearly ultrarelativistic nature of pions in the collisions. The regularities which are observed in analyzing the distributions, irrespectively of the spectrum or the thermal model, are that the π^- -meson temperatures are lower than the proton temperatures and that the Λ temperatures are lower than the proton temperatures.

As we have already indicated, the lower π^- temperatures may be attributed to the presence of a collective motion, which has a stronger effect on the more massive protons than on pions. Given the moderate azimuthal asymmetries, as in Fig. 2, that collective motion must be predominantly azimuthally symmetric, since a significant motion needs to underly the significantly different temperatures. The origin of different temperatures for protons and Λ s is likely tied to the rest-energy cost involved in strangeness production.

Thus, because of the rest-energy cost involved in strangeness production, the strange particles must typically emerge, from their production process, at low velocities relative to their environment. Subsequent interactions may broaden the hyperon spectrum, but not enough to make its width comparable to that of proton spectrum, if the hyperons decouple from the system soon after their production. An early freeze-out for the hyperons may be facilitated by the lower interaction cross-sections with the environment, for the hyperons, than for other baryons. Because of the early freeze-out, the kinetic energies of hyperons

might not tap much, in addition, the energy reservoir represented by the excess rest-energy in baryonic resonance excitations. During system expansion, that excess energy gets converted into the radial collective energy, but some of that conversion may take place only after the Λ s have decoupled from the system. The rest-energy involved in strangeness production taxes also energies of other particles. In a small system such as C + C, some shrinking of spectra can occur and a hint of this may be seen in Table I in that the temperatures for protons and pions are marginally, but systematically, lower in the presence than in the absence of a hyperon, irrespectively of the thermodynamic model employed.

The QGSM has the capability of describing the discussed effects, associated with strangeness energy cost and with interaction cross sections. The results for spectra from the QGSM model are compared to data in Figs. 3, 4 and 5. The temperatures from fits to the QGSM spectra are further compared to those for data in Table I. It is apparent that the model describes adequately the measured spectra. In addition, the model reproduces variation of the temperatures with species and with thermodynamic models fitted to different spectra, and even reproduces the marginal decrease of temperature for associated production.

Elsewhere in the literature, differences in the temperatures of Λ s and protons have been also detected. Thus, in Ni + Cu collisions at 2 AGeV, measured at the Bevalac, the EOS Collaboration [25] has arrived at the Λ temperature of 106 ± 5 MeV and proton temperature of 142 ± 1 MeV, in purely thermal fits to m^\perp -spectra. Analogous fits to spectra from the ARC model [27], for those collisions, gave rise [25] to the temperatures of 91 ± 2 MeV and 121 ± 1 MeV, respectively, for Λ s and protons. In Ni + Ni collisions at 1.93 AGeV, measured at GSI SIS, the FOPI Collaboration [40] has arrived at the temperatures of about 119 MeV and 139 MeV, when fitting m^\perp -spectra of Λ s and of protons, respectively, around midrapidity.

An attempt to separate the collective from thermal motion, for Λ s emitted from central Au + Au collisions at 11.6 AGeV/ c , has been carried out by the E891 Collaboration [41] who have fitted their measured Λ -spectra in terms of an anisotropic blast-wave model. Their fit has produced the temperature of 96 ± 37 MeV in combination with an average radial velocity of $(0.40 \pm 0.12)c$, over the laboratory rapidity range of $(1.7 - 3.2)$. Within errors, those spectral parameters are consistent with those needed to describe the spectra of light nuclei from a very similar central system of Au + Pb at 11.5 AGeV/ c , measured by

the E864 Collaboration [42]. Putting the large errors aside, one should mention that, for a large number of interactions following strangeness production in a large system, there is no principal reason for the Λ and proton temperatures to be very different.

From the measurements of Λ s and of associated yields, for which temperatures got determined, in the same incident-momentum range, we should finally mention the Dubna measurements [43] of Mg + Mg collisions at 4.3 AGeV/ c . The temperatures have been determined there following the Hagedorn model. Rather than from fits to the spectra, however, those temperatures have been inferred from average transverse momenta. For negative pions, the temperatures of 90 ± 1 MeV and 92 ± 2 MeV have been deduced, with and without Λ s, respectively. For Λ s, the temperature of 137 ± 9 MeV has been deduced. The pion temperatures are comparable to those in our measurements. On the other hand, the Λ temperature is significantly higher than ours. Principally, a somewhat stronger radial collective motion in a larger system could be responsible for some increase in temperature for baryons.

VI. SUMMARY

In this paper, we have assessed the characteristics of anisotropic collective flow and spectral temperatures of Λ hyperons emitted from the central C + C collisions at 4.2 AGeV/ c , measured using the Propane Bubble Chamber of JINR at Dubna. In addition, characteristics of protons and of negative pions emitted from those collisions have been determined and provided for comparison.

Directed particle flow has been assessed following the transverse-momentum method of Danielewicz and Odyniec. The Λ hyperons have been found to flow in the same direction as protons and, otherwise, to exhibit the rapidity dependence of in-plane transverse momentum that is quantitatively close to that for protons. The midrapidity flow parameter F was found to take on the value of 99 ± 15 MeV/ c for Λ s and 108 ± 11 MeV/ c for co-produced protons. The similarity of the directed flows for Λ s and co-produced protons contrasts earlier findings of the E895 Collaboration for the Au + Au system at comparable incident momentum, where the Λ flow has been found at least twice as strong as the proton flow.

Elliptic flow in the C + C system, studied around midrapidity, turned out, as the directed flow, to be of the same sign for Λ s and protons and was found to point in the squeeze-out direction, out of the reaction plane. Within errors, the elliptic flow parameters a_2 are

consistent for those particles, at -0.062 ± 0.031 for Λ s and -0.049 ± 0.018 for the co-produced protons.

The spectral temperatures have been determined for Λ s and protons and negative pions produced either in the absence or presence of the Λ -hyperons. Both the c.m.-energy and the transverse energy and momentum spectra have been examined, as well as different variants of the thermodynamic model used to fit data. Lower temperatures have been arrived at for Λ -hyperons and for negative pions than for protons. In addition, the negative-pion temperatures have been found to be a bit lower than the Λ temperatures. A hint of lowering of proton and pion temperatures in the presence of Λ hyperons has been detected.

Experimental results have been compared to the results of collision simulations within the Quark-Gluon String Model which combines string decays with a hadronic interaction cascade. The model describes the observations rather well.

Acknowledgments

The authors are very grateful to N.Amelin for providing them with access to the QGSM code program COLLI. One of the authors (L.Ch.) would like to thank the board of Directors of the Laboratory of High Energies of JINR for the warm hospitality and also thank J. Lukstins and O. Rogachevsky for assistance during the manuscript preparation. This work was partially supported by the U.S. National Science Foundation under Grant Nos. PHY-0555893 and PHY-0800026 and by the Georgian National Science Foundation under Grant GNSF/ST08/4-418.

-
- [1] J. Aichelin *et al.*, Phys. Rev. Lett. **55**, 2661 (1985)
 - [2] W. Weise, Nucl. Phys. A **610**, 35c (1996)
 - [3] C. Sturm *et al.*, Phys. Rev. Lett. **86**, 39 (2001)
 - [4] G. Q. Li *et al.*, Phys. Rev. Lett. **74**, 235 (1995)
 - [5] G. Q. Li *et al.*, Phys. Rev. C **54**, 1897 (1996)
 - [6] G. Q. Li *et al.*, Nucl. Phys. A **636**, 487 (1998)
 - [7] P. Danielewicz *et al.*, Science **298**, 1592 (2002)

- [8] P. Chung *et al.*, Phys. Rev. Lett. 86, 2533 (2001);
C. Pinkenburg *et al.*, Nucl. Phys. A **698**, 495 (2002)
- [9] L. Chkhaidze *et al.*, Yad. Fiz. **67**, 715 (2004) [Phys. At. Nucl. **67**, 693 (2004)]
- [10] L. Chkhaidze *et al.*, Phys. Lett. B **411**, 26 (1997)
- [11] L. Chkhaidze *et al.*, Phys. Lett. B **479**, 21 (2000)
- [12] N. Amelin *et al.*, Yad. Fiz. **51**, 512 (1990) [Sov. J. Nucl. Phys. **51**, 327 (1990)]; *ibid.* **52**, 272 (1990), [Sov. J. Nucl. Phys. **52**, 172 (1990)]
- [13] N. Amelin *et al.*, Phys. Rev. Lett. **67**, 1523 (1991)
- [14] A. Bondarenko *et al.*, JINR Preprint P1-98-292, Dubna, (1998), http://cedb4fs.kek.jp/cgi-bin/img_index?9905017
- [15] G. N. Agakishiev *et al.*, Yad. Fiz. **43**, 366 (1986) [Sov. J. Nucl. Phys. **43**, 234 (1986)]; E. Kladnitskaya and K. Iovchev, JINR Report P1-86-166, Dubna (1986)
- [16] P. Danielewicz and G. Odyniec, Phys. Lett. B **157**, 146 (1985)
- [17] P. Danielewicz *et al.*, Phys. Rev. C **38**, 120 (1988)
- [18] J. Lukasik and W. Trautmann, arXiv: nucl-ex/0603028v1 (2006)
- [19] O. Beavis *et al.*, Phys. Rev. C **33**, 1113 (1986)
- [20] W. Wilson *et al.*, Phys. Rev. C **45**, 738 (1992)
- [21] P. Jain, G. Singh and A. Mukhopadhyay, Phys. Rev. Lett. **74**, 1534 (1995)
- [22] M. Adamovich *et al.*, Eur. Phys. J. A **2**, 61 (1998); Eur. Phys. J. A **6**, 427 (1999); Yad. Fiz. **67**, 290,(2004)
- [23] K. G. Doss *et al.*, Phys. Rev. Lett. **57**, 302 (1986)
- [24] J. L. Ritman *et al.*, Z. Phys. A **352**, 355 (1995)
- [25] M. Justice *et al.*, Phys. Lett. B **440**, 12 (1998)
- [26] H. Liu *et al.*, Phys. Rev. Lett. **84**, 5488 (2000)
- [27] Y. Pang, T. J. Schlagel and S. H. Kahana, Phys. Rev. Lett. **68**, 2743 (1992)
- [28] H. Sorge, Phys. Rev. C **52**, 3291 (1995)
- [29] L. Chkhaidze *et al.*, Nucl. Phys. A **794**, 115 (2007)
- [30] N. Amelin *et al.*, JINR Preprint P2-86-837 (Dubna, 1986)
- [31] H. Heiselberg and A.-M. Levy, Phys. Rev. C **59**, 2717 (1999)
- [32] C. Pinkenburg *et al.*, Phys. Rev. Lett. **83**, 1295 (1999)
- [33] A. Andronic *et al.*, Nucl. Phys. A **679**, 765 (2001)

- [34] S. Nagamiya *et al.*, Phys. Rev. Lett. **49**, 1383 (1982)
- [35] R. Stock, Phys. Rep. **135**, 261 (1986)
- [36] J. Kapusta, Phys. Rev. C **16**, 1493 (1977)
- [37] R. Hagedorn, in *Cargese Lectures in Physics*, vol. VI, ed. E. Schatzmann (Gordon and Breach, New York, 1973)) p. 643
- [38] R. Hagedorn, Suppl. Nuovo Cimento **3**, 147 (1965); R. Hagedorn and J. Ranft, Suppl. Nuovo Cimento **6**, 169 (1968); R. Hagedorn R. and J. Rafelski, Phys. Lett. B **97**, 136 (1980); R. Hagedorn, Nuovo Cimento Riv. **6**, 1 (1983); R. Hagedorn, CERN Preprint, CERN-TH-3918, 1984
- [39] I. Gradstein and I. Rizik, *Tables of Integrals, Sums and Rows* (Nauka, Moscow, 1971) p. 981
- [40] M. Merschmeyer *et al.*, Phys. Rev. C **76**, 024906 (2007)
- [41] S. Ahmad *et al.*, Nucl. Phys. A **636**, 507 (1998)
- [42] T. A. Armstrong *et al.*, Phys. Rev. C **61**, 064908 (2000).
- [43] S. Avramenko *et al.*, Yad. Fiz. **55**, 721 (1992) [Sov. J. Nucl. Phys. **55**, 400 (1992)]

List of Tables

- I The temperatures of Λ -hyperons, and of protons and π^- mesons, produced either in the presence or absence of Λ s, inferred from different spectra following different thermal-model assumptions discussed in the text.

20

List of Figures

- 1 Average component of transverse momentum in the reaction plane, as a function of c.m. rapidity, for Λ hyperons in panel (a), and for protons co-produced with the Λ s in panel (b). The data from central C + C collisions at 4.2 AGeV/c, corrected for $\langle \cos \Phi \rangle$, are represented by circles. Results from simulations in the QGSM model are represented by crosses. The straight-line stretches represent the slopes of the data at midrapidity cross-over and result from fitting the data with an odd third-order polynomial within the rapidity region of $|y| < 0.65$ for (a), and $|y| < 0.70$ for (b). The curved lines guide the eye over data. 21

2	<p>Distribution of midrapidity Λs (a), and of co-produced protons (b), in the azimuthal angle with respect to the estimated reaction plane, in the C + C collisions at 4.2 AGeV/c. The Λ hyperons stem from the rapidity region of $y < 0.65$ and the protons stem from $y < 0.70$. The circles represent data. The crosses represent results of QGSM, with the normalization set to match that of the data. The lines represent fits to the data with the function $dN/d\varphi = a_0 (1 + a'_1 \cos \varphi + a'_2 \cos 2\varphi)$.</p>	22
3	<p>Spectra of Λ-hyperons emitted from C + C collisions, at $y < 0.6$: (a) distribution of Λs in the transverse momentum, (b) scaled distribution of Λs in the c.m. kinetic energy, and (c) scaled distribution of Λs in the transverse mass. Circles represent data and stars represent QGSM results. Lines represent thermal fits to the data, discussed in the text.</p>	23
4	<p>Spectra of protons produced in the presence (a,b,c) or absence (d,e,f) of Λ hyperons, at $y < 0.6$. The leftmost panels (a,d) show the distribution of protons in the transverse momentum, the center panels (b,e) show the scaled distribution of protons in the c.m. kinetic energy, and the rightmost panels (c,f) show the scaled distribution of protons in the transverse mass. Circles represent data and stars represent QGSM results. Lines represent thermal fits to the data, discussed in the text.</p>	24
5	<p>Spectra of π^- mesons produced in the presence (a,b,c) or absence (d,e,f) of Λ hyperons, at $y < 0.8$. The leftmost panels (a,d) show the distributions of mesons in the transverse momentum, the center panels (b,e) show the scaled distributions of mesons in the c.m. kinetic energy, and the rightmost panels (c,f) show the scaled distributions of mesons in the transverse mass. Circles represent data and stars represent QGSM results. Lines represent thermal fits to the data, discussed in the text.</p>	25

TABLE I: The temperatures of Λ -hyperons, and of protons and π^- mesons, produced either in the presence or absence of Λ s, inferred from different spectra following different thermal-model assumptions discussed in the text.

Particles	Spectrum Origin	Number of Particles	Spectral Temperature T (MeV) for		
			dN/dp^\perp	dN/dE_K	dN/dm^\perp
Λ $ y < 0.6$	Data	561	105 ± 7	111 ± 7	103 ± 6
	QGSM	7578	106 ± 3	105 ± 3	102 ± 3
p with Λ $ y < 0.6$	Data	3961	135 ± 5	132 ± 4	128 ± 4
	QGSM	33653	133 ± 3	128 ± 3	129 ± 3
p , no Λ $ y < 0.6$	Data	76002	140 ± 3	136 ± 3	134 ± 3
	QGSM	213560	136 ± 2	133 ± 2	130 ± 2
π^- with Λ $ y < 0.8$	Data	1146	94 ± 2	85 ± 2	81 ± 2
	QGSM	12005	93 ± 2	88 ± 2	81 ± 2
π^- , no Λ $ y < 0.8$	Data	23781	98 ± 2	86 ± 2	85 ± 2
	QGSM	66820	96 ± 2	90 ± 2	84 ± 2

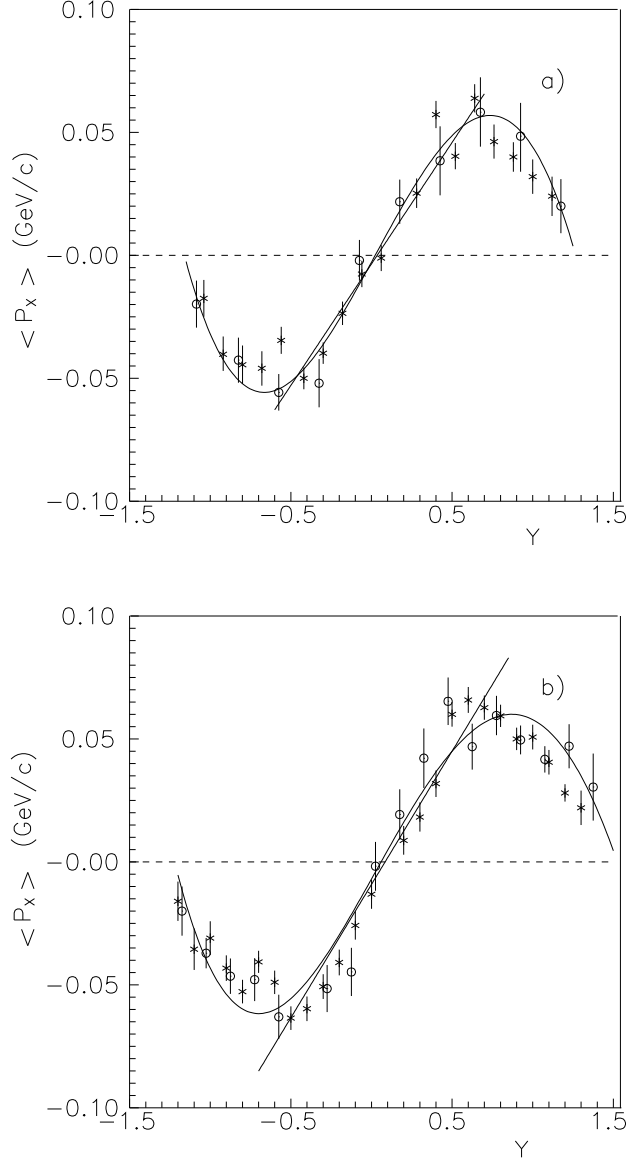


FIG. 1: Average component of transverse momentum in the reaction plane, as a function of c.m. rapidity, for Λ hyperons in panel (a), and for protons co-produced with the Λ s in panel (b). The data from central C + C collisions at 4.2 AGeV/c, corrected for $\langle \cos \Phi \rangle$, are represented by circles. Results from simulations in the QGSM model are represented by crosses. The straight-line stretches represent the slopes of the data at midrapidity cross-over and result from fitting the data with an odd third-order polynomial within the rapidity region of $|y| < 0.65$ for (a), and $|y| < 0.70$ for (b). The curved lines guide the eye over data.

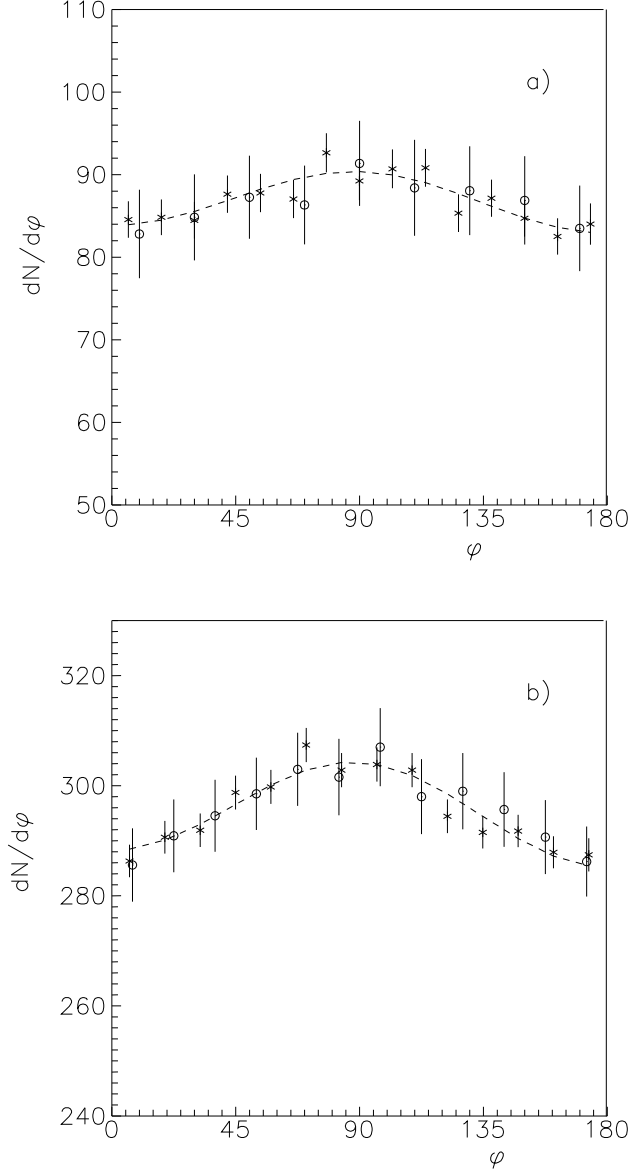


FIG. 2: Distribution of midrapidity Λ s (a), and of co-produced protons (b), in the azimuthal angle with respect to the estimated reaction plane, in the C + C collisions at 4.2 AGeV/c. The Λ hyperons stem from the rapidity region of $|y| < 0.65$ and the protons stem from $|y| < 0.70$. The circles represent data. The crosses represent results of QGSM, with the normalization set to match that of the data. The lines represent fits to the data with the function $dN/d\varphi = a_0 (1 + a'_1 \cos \varphi + a'_2 \cos 2\varphi)$.

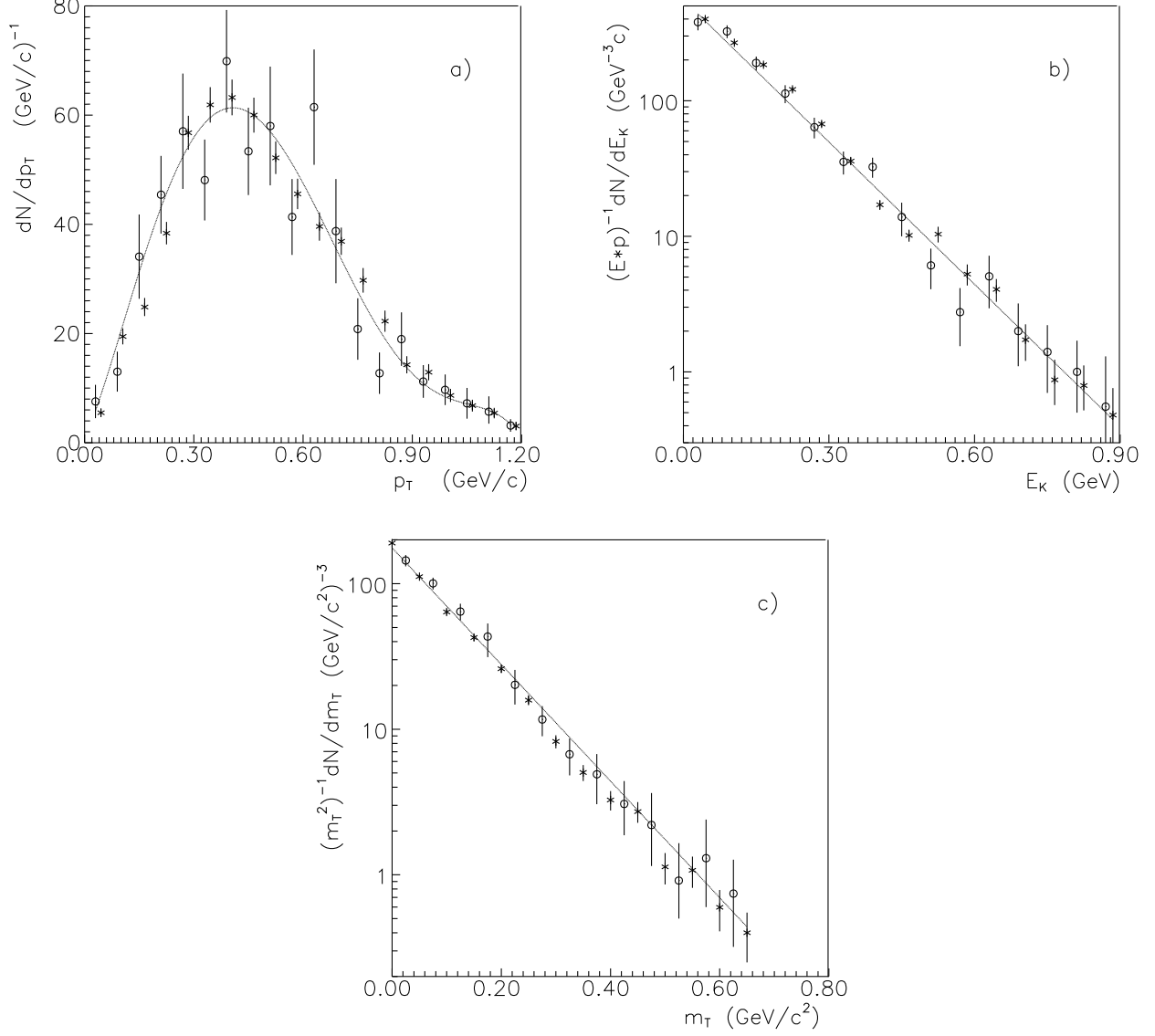


FIG. 3: Spectra of Λ -hyperons emitted from C + C collisions, at $|y| < 0.6$: (a) distribution of Λ s in the transverse momentum, (b) scaled distribution of Λ s in the c.m. kinetic energy, and (c) scaled distribution of Λ s in the transverse mass. Circles represent data and stars represent QGSM results. Lines represent thermal fits to the data, discussed in the text.

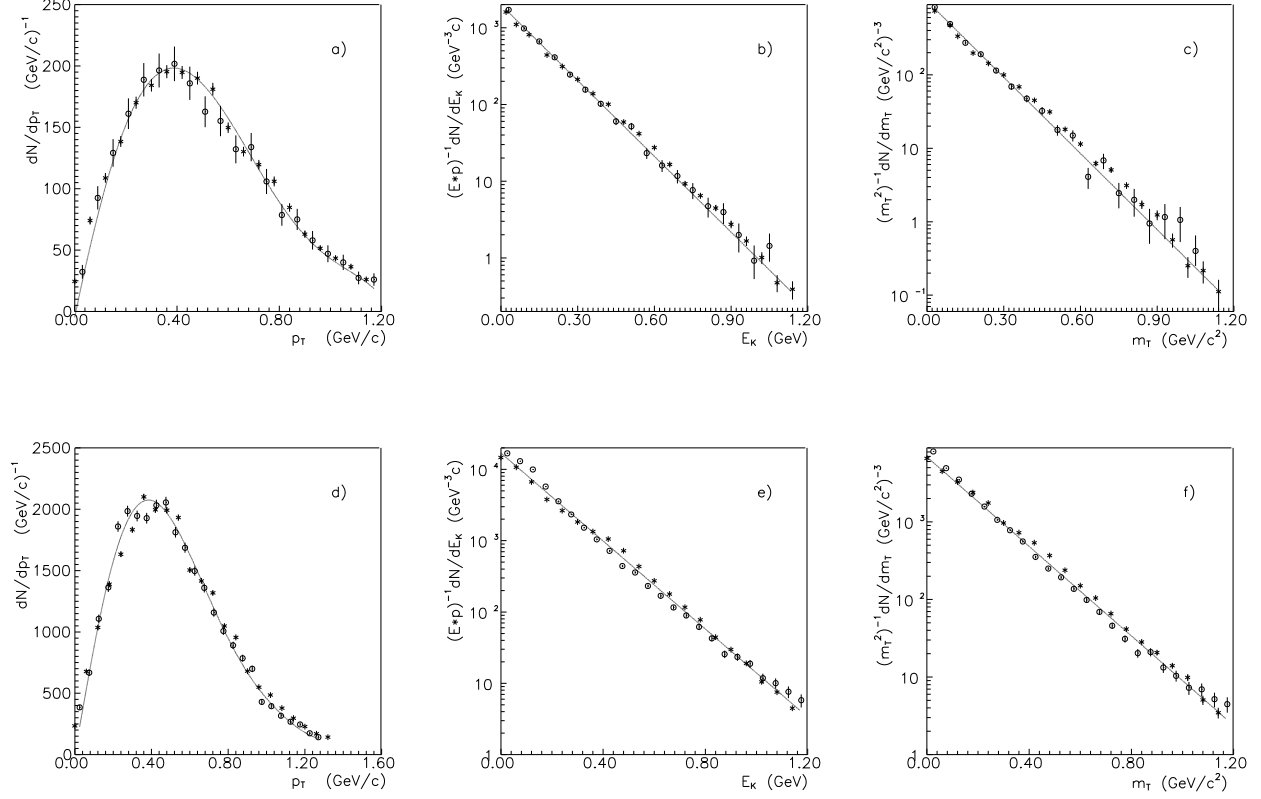


FIG. 4: Spectra of protons produced in the presence (a,b,c) or absence (d,e,f) of Λ hyperons, at $|y| < 0.6$. The leftmost panels (a,d) show the distribution of protons in the transverse momentum, the center panels (b,e) show the scaled distribution of protons in the c.m. kinetic energy, and the rightmost panels (c,f) show the scaled distribution of protons in the transverse mass. Circles represent data and stars represent QGSM results. Lines represent thermal fits to the data, discussed in the text.

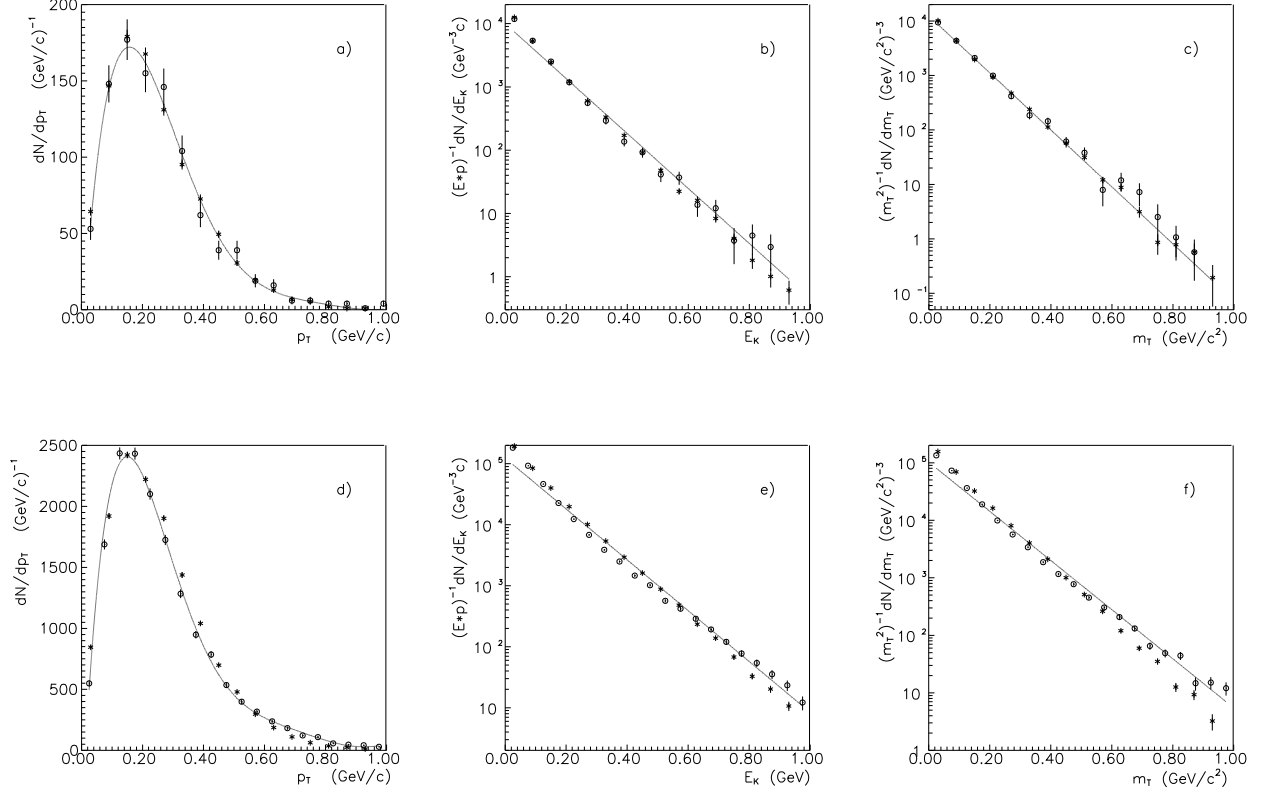


FIG. 5: Spectra of π^- mesons produced in the presence (a,b,c) or absence (d,e,f) of Λ hyperons, at $|y| < 0.8$. The leftmost panels (a,d) show the distributions of mesons in the transverse momentum, the center panels (b,e) show the scaled distributions of mesons in the c.m. kinetic energy, and the rightmost panels (c,f) show the scaled distributions of mesons in the transverse mass. Circles represent data and stars represent QGSM results. Lines represent thermal fits to the data, discussed in the text.